Journal of Archaeological Science: Reports 9 (2016) 87–93

Contents lists available at ScienceDirect

Journal of Archaeological Science: Reports

journal homepage: www.elsevier.com/locate/jasrep

The use of close-range photogrammetry in zooarchaeology: Creating accurate 3D models of wolf crania to study dog domestication

Allowen Evin [a,b,c,*], Thibaud Souter [b], Ardern Hulme-Beaman [b,c], Carly Ameen [b,c], Richard Allen [d], Pietro Viacava [e], Greger Larson [d], Thomas Cucchi [e,b], Keith Dobney [b,c]

[a] Institut des Sciences de l'Evolution, Université de Montpellier, CNRS, IRD, EPHE, Place Eugène Bataillon, 34095 Montpellier Cedex 05, France
[b] Department of Archaeology, University of Aberdeen, St. Mary's Building, Elphinstone Road, Aberdeen, UK
[c] Department of Archaeology, Classics and Egyptology, University of Liverpool, 12-14 Abercromby Square, Liverpool, L69 7WZ, UK
[d] Palaeogenomics & Bio-Archaeology Research Network, Dyson Perrins Building, South Parks Road, Oxford OX1 3QY, UK
[e] CNRS-Muséum National d'Histoire Naturelle, UMR 7209, Archéozoologie, Archéobotanique Sociétés, Pratiques et Environnement, 55 rue Buffon, 75005 Paris, France

ARTICLE INFO

Article history:
Received 17 February 2016
Received in revised form 29 May 2016
Accepted 14 June 2016
Available online xxxx

Keywords:
Geometric morphometrics
Skull
Canis lupus
Wolf
Surface scanning
3D models
Photogrammetry

ABSTRACT

Close-range photographic techniques - including photogrammetry - are becoming common tools for constructing three-dimensional (3D) models of artifacts, particularly in archaeological research. Whether models obtained through photogrammetry can be used for zooarchaeological studies requires a systematic examination. In the context of research into dog domestication, we explore whether 3D models of wolf crania, obtained through a photogrammetric approach, accurately describe the original cranium in term of colouration, texture and most importantly, geometry.

To answer this question, we compared the topology of 3D models obtained with a high-resolution surface scanner (used as reference geometry) with models reconstructed from the same five wolf crania using photogrammetry. The pairs of models were then compared using both a visual, qualitative and two quantitative approaches. The latter, a geometric comparison computed the deviation map between the pairs of 3D models, which was then followed by a 3D landmark based geometric morphometric approach using corresponding analyses.

Our results demonstrate that photogrammetry can produce 3D models with visually satisfying levels of morphological detail in terms of texture, colouration and geometry. In addition, the quantitative comparison of the models revealed an average distance between the two surfaces of 0.088 mm with an average standard deviation of 0.53 mm. The geometric morphometric analyses revealed the same degree of measurement error for the two series of scans (2.04% and 1.95%), with only 6.31% of the morphometric variation being due to the acquisition technique. Photogrammetry, therefore, offers a low cost, easily portable and simple to perform alternative to traditional surface scanning, affording advantages that make it a highly useful tool for zooarchaeological research.

1. Introduction

Image-based 3D modeling has grown significantly over the last decade, offering new possibilities for recording archaeological artifacts (e.g. Counts et al. 2016, Grosman et al., 2008; Haukaas and Hodgetts, 2016, Mcpherron et al., 2009; Pavlidis et al., 2007; Porter et al., 2016). Whilst surface scanning technology has revolutionised the acquisition of 3D models, it remains relatively expensive and not always readily portable. As a consequence, the more traditional techniques of photogrammetry have recently experienced a resurgence of interest. Beginning in the mid-nineteenth century, photogrammetry has been used intensively in a geographic context - in particular for applications related to cartography, survey, spatial planning and geomorphological analyses (e.g. Núñez et al., 2013; Verhoeven et al., 2012; Sapirstein, 2016; Yamafune et al., 2016). Driven by technical developments for the surface digitisation of objects using close-range techniques over the last 15 years, photogrammetry is now becoming a common tool in archaeological research. These close-range techniques of photogrammetry have the distinct advantage over other 3D model building methods - being both cheap and portable, requiring only a conventional camera and minimal accompanying equipment and setup.

In parallel with the rapid development and use of 3D model acquisition, geometric morphometric approaches are also increasingly being applied to address bioarchaeological questions (e.g. Bouby et al., 2013; Cucchi et al., 2011, 2013, 2014; Evin et al., 2013, 2014; Newton et al., 2014; Pagnoux et al., 2014; Ros et al., 2014; Seetah

* Corresponding author at: Institut des Sciences de l'Evolution, Université de Montpellier, CNRS, IRD, EPHE, Place Eugène Bataillon, 34095 Montpellier Cedex 05, France.
E-mail address: allowen.evin@univ-montp2.fr (A. Evin).

http://dx.doi.org/10.1016/j.jasrep.2016.06.028

et al., 2012; Terral et al., 2010). Geometric morphometrics are employed to measure and analyse the size and shape of objects using coordinates taken from specific, homologous locations – i.e. landmarks – or along curves and surfaces – i.e. 2D and 3D sliding semi-landmarks (Bookstein, 1997; Gunz and Mitteroecker, 2013; Gunz et al., 2005; Souter et al., 2010). Coordinates of these landmarks can be obtained from 3D models, but these measurements are only valid if the said model's accurately retains the geometry of the physical object studied. In addition, rendering both colour and texture onto these models can aid accurate identification of the desired landmarks.

Photogrammetry relies on partially overlapping digital photographs taken from multiple angles to reconstruct the three-dimensional topology of the external, visible surface of an object of interest. The reconstructed 3D coordinates form a 'point cloud' that can then be triangulated - forming a 3D mesh that can be rendered as a polygonal model.

Studies combining both photogrammetry and geometric morphometrics are rare - mostly limited to the fields of anthropology (Friess, 2012; Katz and Friess, 2014; Hassett and Lewis-Bale, 2016) and medicine (e.g. Weinberg et al., 2009). In addition, the accuracy with which photogrammetry preserves the geometry of objects, for subsequent morphometric analyses, requires further examination. In 2014, Katz and Friess assessed the suitability of photogrammetry as a tool for capturing and quantifying the morphology of the human crania by comparing 3D models obtained through a photogrammetric protocol and a high precision scanner. Katz and Friess (2014) found a low degree of deviation, with surface area measurements slightly larger for photogrammetry models. In that study, a geometric morphometric analysis revealed larger cranial shape differences between individuals than between the technologies used to construct the models, thereby confirming the appropriateness of combining photogrammetry with geometric morphometrics. Its generalization to other mammalian taxa and to other photogrammetric protocols now remains to be tested.

Our research focuses on animal domestication, which is both a complex and dynamic field pertaining to the more recent bio-cultural history of humans. It is generally accepted that the first domesticate was the dog, which entered the human sphere long before the domestication of other plants and animals. The timing and location of dog domestication from their wolf ancestors remains controversial, with the most ancient canids identified as 'domestic' from either contextual or morphological criteria (Boudadi-Maligne and Escarguel, 2014). In most cases of animal domestication, a number of morphological changes occurred. These morphological changes are traditionally used as criteria for distinguishing between wild and domestic forms, and often include a reduction in size, especially of the skull (e.g. Davis, 1981; Morey, 1992; Tchernov and Kolska Horwitz, 1991). However, when attempting to separate e.g. wolves and dogs, several studies have stressed the need for analysing not only the size of the cranium, but also its shape, (Boudadi-Maligne and Escarguel, 2014; Drake et al., 2015; Wayne, 1986).

The anatomical complexity of the cranium is challenging for surface reconstruction methods, as it possesses significant topological detail of a diverse scale and nature, including concavities, openings and distinctive biological landmarks of various kinds. Therefore, in order to assess whether photogrammetry can precisely reconstruct high-resolution, and geometrically accurate, 3D models for use in geometric morphometric analyses, we compared 3D models of five modern wolf crania obtained through i) photogrammetry and ii) high-end structured light surface scanning used as a reference for 'true' geometry. The pairs of models were compared using both a visual qualitative approach and two quantitative methods - firstly by computing the deviation map between the pairs of 3D models and secondly using a landmark based geometric morphometric approach and corresponding analyses.

2. Material and methods

The five specimens of wolf crania included in this study are housed in the collections of the Muséum National d'Histoire Naturelle (Paris, France) – specimens numbered MNHN-ZM-AC-1997-12, MNHN-ZM-MO-1996-2499, MNHN-ZM-MO-1997-452, MNHN-ZM-MO-1997-453 and MNHN-ZM-MO-1997-454.

2.1. Scanner and photogrammetric reconstructions

2.1.1. Scanner-based 3D models

The scanner-based 3D models were generated using a Breuckmann StereoScan structured light scanner (http://www.breuckmann.com). Considering the size of the objects, the scanner was mounted with the medium-range of optical lenses, offering a diagonal scope of 250 mm and an average spatial precision of 18 μm. The data acquisition was performed using its dedicated software Optocat (http://www.breuckmann.com) coupled to its automated turntable. In this set-up, a complete specimen scan was obtained in two successive full rotations, each with 12 stops per-pass. The crania were successively positioned vertically (with the rostrum pointing upward) and horizontally (with the cranium lying on the lateral side) on the turntable. The 2×12 set of 3D views was semi-automatically aligned along the scanning process, before being fused into a single mesh and exported as a .PLY file. The mesh was then cleaned using Geomagic (www.geomagic.com) in order to assure it did not present any major geometric inconsistencies (i.e. noise, holes or intersecting, abnormal or non-manifold faces).

2.1.2. Photogrammetric-based 3D models

Photogrammetry reconstructs 3D models from a set of photographs taken from various angles. These images must cover the entire surface of the object with significant overlap between pairs of photographs. The images were acquired in a large room offering a very abundant and diffuse light source that reduced the presence of glare or directional, harsh cast-shadows on the object. We used an 8 mega-pixel digital single-lens reflex (DSLR) Canon EOS 30D camera, mounted with a Canon EF 24–105 mm f/4 L IS USM lens. With each cranium placed successively on a small central desk, the photographs were shot at regular intervals of approximately 10°, as the operator moved the tripod-mounted camera around in a circle (Fig. 1A). To ensure proper convergence of the orientation algorithms, photographs were centred primarily on the object of interest, whilst also including a fair amount of the surroundings in the frame (approximately 2/3rds of the image) - with much of it within the depth-of-field and an aperture stop set at f/16. The crania were set on a rigid, planar cardboard sheet displaying a calibrated referential pattern (Fig. 1B). This pattern provided a visual aid for 10-degree increments, as well as unambiguous feature points for image orientation and (essentially) fixed dimension geometry to scale the 3D models for later geometrical comparison. Sets of 36 pictures were acquired from three different vertical angles (approximately 0°, 15° and 40°; see Fig. 1A) for both the dorsal and the ventral sides of each cranium, which were later scaled and digitally re-assembled into a single object. Therefore, a total of 216 ($36 \times 3 \times 2$) pictures were used to reconstruct each model.

Each dorsal and ventral sets of 108 images were imported into VisualSFM for photogrammetric processing (Wu, 2011). This freeware allowed us to perform keypoint detection (unambiguous feature-points in each image) through SIFT algorithms (i.e. Scale Invariant Feature Transforms; Lowe, 1999; Wu, 2007), tie-points matching (matching points between pairs of photographs), sparse 3D points generation (Sholts et al., 2011; Wu, 2013; Wu et al., 2011) and finally to reconstruct high-resolution 3D point-clouds by dense correlation through CMVS-PMVS algorithms (i.e. Clustering Views for Multi-view Stereo and Patch Based Multi-view Stereo Software; Furukawa and Ponce, 2010). For each specimen, two dense 3D point clouds (one for the ventral and one for the dorsal view of the cranium) were saved as .PLY files. These dense point clouds required substantial manual cleaning before

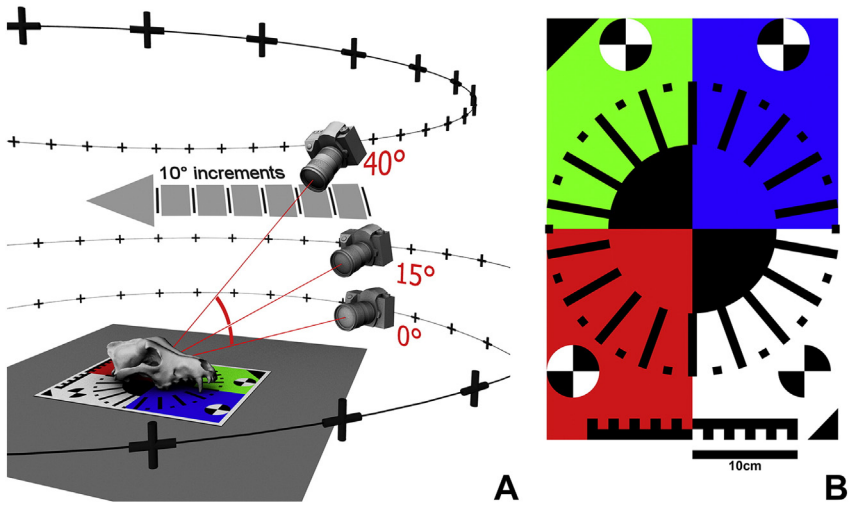

Fig. 1. A: schematic representation of the set-up and camera positions used for the acquisition of the photographs. B: fixed dimensions reference pattern used to scale the models and enhance the performance of key-points detection/matching and camera calibration algorithms.

being triangulated, and the resulting meshes were scaled to the actual dimension of the object using Geomagic. The two cranium halves were then aligned, using a least-square optimisation best-fit alignment, before being fused into a single 3D model that then underwent a final cleaning procedure to warrant its geometric consistency.

N.B. After this study, new semi-automated and automated protocols, requiring much less room and fewer operator interventions, were designed and implemented for image acquisition, providing models of comparable quality, whilst drastically reducing the amount of time needed to acquire the photographs (see SI-text and Supplementary Fig. 1).

2.2. 3D models comparisons

A first comparison of the pairs of models includes: 1) a visual observation of the models, and 2) the computation of a mesh-to-mesh deviation map. The pairs of models were spatially aligned (using a least-square optimisation best-fit alignment) in order to compare their 3D topology. We computed the local distance for each 3D point between a 'reference geometry' (here the structured light scanner model) and a 'test geometry' (here the photogrammetric model) and retrieved the average distance and the standard deviation values.

A second analysis compared the geometric accuracy of the two acquisition protocols with a three dimensional landmark based geometric morphometric approach. This landmark approach involved recording a set of 28 3D-landmarks on the 10 models using a protocol adapted from Drake and Klingenberg (2008) (Supplementary Fig. 2). Landmark coordinates were recorded, five times per specimen, using 'Landmark Editor' (http://graphics.idav.ucdavis.edu/research/EvoMorph) and superimposed using a Generalized Procrustes Analysis (Goodall, 1995; Rohlf and Slice, 1990) and the right and left sides of the crania were symmetrized (Kolamunnage and Kent, 2003). The variation in shape was synthesized using a Principal Component Analysis (PCA), and the shape differences associated with the PCA axes visualised using multivariate regressions (Monteiro, 1999). In order to assess the error linked with the landmark digitisation process, Procrustes Anovas were performed for data acquired on the Breuckmann and photogrammetric models separately, with individual as the factor. Then, the five replicates per model were averaged and a Procrustes Anova performed, again with individual as the factor, in order to quantify the part of the variation linked to the scanning technique. Procrustes

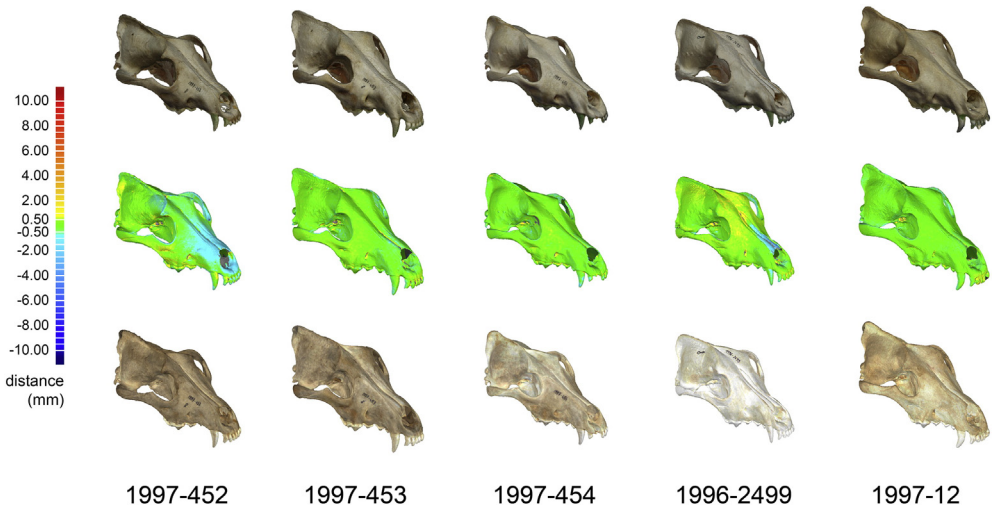

Fig. 2. Models obtained with photogrammetry (top) and the Breuckmann structured light scanner (bottom) with the cloud-mesh distances visualisation (middle). Differences are expressed using the colour scale on the left. (For interpretation of the references to colour in this figure legend, the reader is referred to the web version of this article.)

Anovas were also performed to test differences between the scanning techniques for each of the specimens independently, and a two-way Anova was used to assess the homogeneity of the results obtained with the two techniques (using individual and acquisition technique as factors).

All the analyses were performed using the Geomorph (Adams and Otárola-Castillo, 2013) and Rmorph (Baylac, 2012) packages for 'R' (R Core Team, 2014).

3. Results

Both the scannographic and photogrammetric models succeeded in producing 3D models that displayed visually satisfying levels of morphological detail in terms of texture, colouration and geometry (3D models are provided as supplementary files). The capture and rendering of topological detail was good and appeared similar in all pairs of 3D models (Fig. 2), except when viewing the tooth row. In the latter case, the Breuckmann models presented higher resolution of fine details, rendered with greater consistency (Fig. 3). The surface scanner produces the colour texture by equalising and averaging pictures taken at each stop of its turn-table with its internal camera and projector light and this tends to produce soft contrast, low-fidelity colour mapping that blends and softens minor local details like bone sutures and other marks. In contrast, photogrammetric models are produced with constant illumination and reconstruction algorithms that preserve a very high amount of radiometric fidelity and consistency.

The mesh-to-mesh distance comparisons reveal a high level of similarity in the geometry of the models, with most of the differences being very small - generally below 0.5 mm (Fig. 2). The only areas that differ more markedly between the pairs of models (in red or dark blue) lie either within the nasal cavity or occipital foramen. Such highly concave zones like these are admittedly considered less visible and thus inaccessible to surface reconstruction methods and are not included in comparative morphometric (including geometric morphometrics) studies. The quantitative comparison of the models revealed an average distance between the two surfaces of 0.088 mm (min: 0.04 mm, max: 0.17 mm), with an average standard deviation of 0.53 mm (min: 0.47 mm, max: 0.61 mm) (Table 1).

The first two axes of the PCA computed on the shape data represented 75.21% of the total variance. Along these two axes - respectively 47.58% and 29.16% of the variance explained - the two acquisition methods greatly overlapped with nearly the same range of variation, and with the measurements of each specimen showing no overlap (Fig. 4). Here, individuals differ mainly in the shape of the posterior part of the cranium, with the specimens in the negative side of the axes (in grey) showing proportionally broader brain case and zygomatic arches (Fig. 4). However, differences in scanning technologies were visible for at least three of the specimens (MNHN-ZM-MO-1997-453, MNHN-ZM-MO-1997-454 and especially MNHN-ZM-MO-1997-452), for which measurements corresponding to the photogrammetry model do not overlap with measurements acquired with the Breuckmann scanner (Fig. 4). Procrustes Anovas revealed strong differences between the specimens ($p = 0.01$) but not between the scanning techniques ($p = 0.726$). For each specimen, the measurements strongly differ between the two scanning technologies (all $p < 0.01$), but the differences are homogeneous among specimens ($p = 0.984$) even if the shape differences are localised in different areas of the cranium (Supplementary Fig. 2). The landmark digitisation error for the Breuckmann models is 2.04%, and 1.95% for the Photogrammetric models and 6.31% of the variation is explained by the scanning technique.

4. Discussion

Our data revealed that photogrammetry can be an accurate tool to reconstruct 3D models of wolf crania in terms of both geometry and appearance, and can, therefore, provide an equally good alternative to other more common means of 3D surface digitisation including structured light or laser scanners. Photogrammetry is also relatively inexpensive - only requiring a standard digital camera and freely distributed software (except Geomagic that can be replaced by other software including e.g. Meshlab (Cignoni et al., 2008)).

Photogrammetric 3D models are also relatively easy to obtain, since protocols for data acquisition are available and discussed in the literature (Bates et al., 2010; Falkingham, 2012; Katz and Friess, 2014). In addition, tutorials explaining the entire process from photographs to 3D models are freely available online.

Given its lack of expense, portability and simplicity, photogrammetry offers a very promising tool for geometric morphometric studies of zooarchaeological specimens. High-end digital cameras and simple lighting equipment are readily available and commonly used in institutions for the conservation of cultural heritage and are routinely included as part of a researcher's equipment when visiting remote field locations or other institutional collections.

Photogrammetry also has the advantage of being inherently portable, as the camera is usually small and durable, and carries its own battery power supply – all very important assets when working either in the field, in remote areas or in places offering a limited or unreliable power supply. A significant advantage when targeted specimens cannot be transported (e.g. because of their weight, size, importance administrative obstacles and time involved in processing loan permissions).

Another major advantage of photogrammetry is its potential for performing data acquisition (photographs) as a quick and separate step from the 3D data reconstruction, a feature currently not offered by most surface scanners. This benefit significantly reduces the time devoted to digitisation and thus maximizing the number of models that can be collected during sessions. As an example, in our study the acquisition of all the pictures required for the 3D reconstructions could be performed in approximately fifteen minutes, compared with the forty-five minutes required on average by the structured light surface scanner we used.

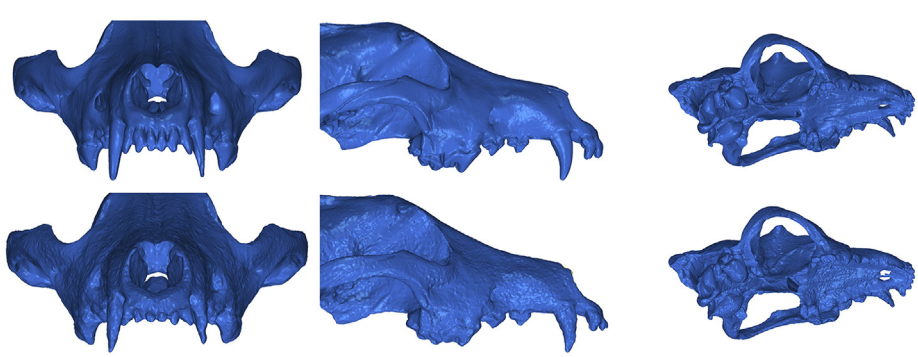

Fig. 3. Detailed views of 3D models of specimen MNHN-ZM-MO-1997-452 obtained with the Breuckmann structured light scanner (left) and photogrammetry (right).

Table 1
Quantitative comparison of the 3D models obtained with photogrammetry and the Breuckmann scanner. The measurements are in millimeters.

	1997–452	1997–453	1997–454	1996–2499	1997–12
Average distance	0.11	0.07	0.05	0.17	0.04
Standard deviation	0.52	0.49	0.61	0.47	0.57

One should consider all trade-offs between both technologies, however. The surface scanning time includes the 3D reconstruction, triangulation and fusion steps, and results in a single, relatively more detailed mesh (especially along the tooth row), which requires only very limited manual cleaning and processing and no scaling before being incorporated in the analysis. In contrast, the photogrammetric procedure includes several additional steps, involving substantial computation time and heavier manual intervention before the raw images are turned into an operable 3D model. Ultimately, we consider these drawbacks, though potentially significant, are largely compensated for by the benefits photogrammetry offers in terms of ease of use, cost, acquisition time, accessibility and maneuverability in most situations pertaining to the field of archaeological sciences.

Photogrammetry is commonly used in archaeology to construct 3D models of architectural structures, archaeological sites, landscapes or artifacts. In this study we demonstrate that photogrammetry is also a promising tool for geometric morphometric (GM) studies, revealing that GM variation between specimens greatly exceeded the variation produced by the other scanning technology used - with reasonable uncertainty shown between the two techniques (6.31% of total variation). Several studies, exploring the possibility of combining 3D coordinates measured directly on specimens (using for example a microscribe) with coordinates measured on 3D models obtained from various sources (e.g. CT-Scans, laser or structured light scanners) (e.g. Badawi-Fayad and Cabanis, 2007; Sholts et al., 2011 for CT-Scans/microscibe comparisons) have found relatively good congruence between coordinates obtained from various sources that were sufficiently good to enable geometric morphometric analyses, - although some differences were observed depending of the type of landmark analysed and the experience of the operator. All studies combining such data should be performed with caution (Sholts et al., 2011) and require careful examination of the potential bias prior to any geometric morphometric analyses.

5. Conclusion

Results show that photogrammetric 3D models, obtained through a relatively fast and easy-to-operate acquisition protocol - used with freely distributed software in default mode, can offer geometric and texturally accurate results as good as the highest-end surface scanners currently used in cultural and natural heritage research facilities. We demonstrate how closely these photogrammetric models match the original object and argue that such an approach is ideally suited to running landmark based geometric morphometric analyses, yielding measurements that are directly comparable to those performed on the scannographic models.

We found the surface scanner retained some advantages, but only in a limited set of areas displaying particularly fine and intricate topological details – e.g. such as the tooth row. However, these minimal differences, which were not the primary focus of our study and do not

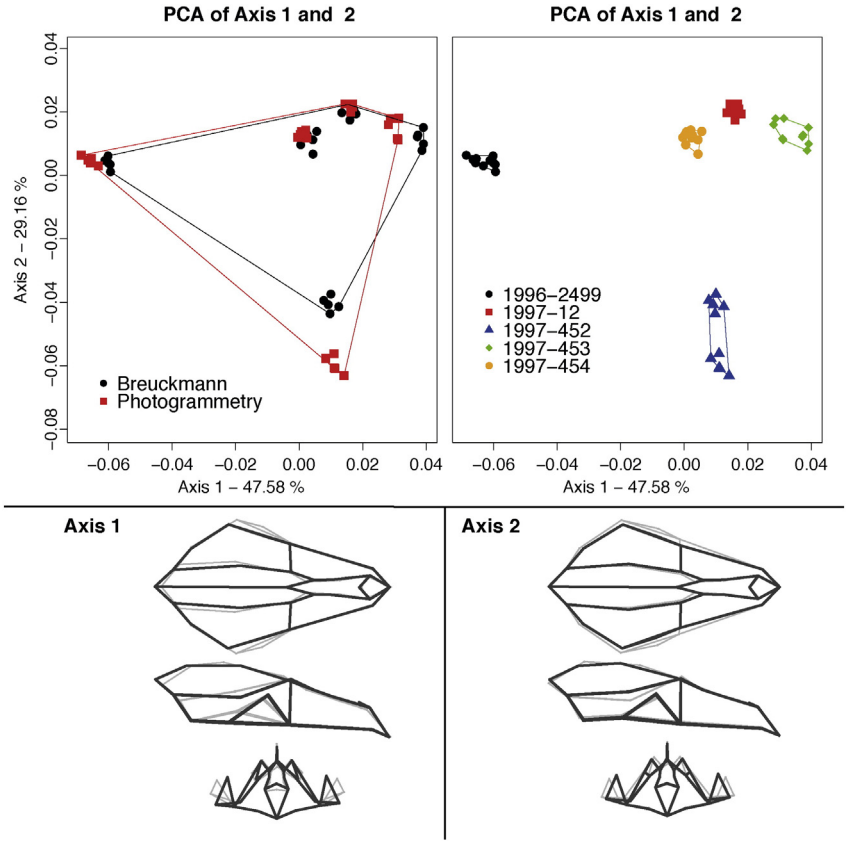

Fig. 4. Top: Two first axes of the PCA showing variation between scanning technic (left) and specimens (right). Bottom: Shape differences along the first (left) and second (right) PCA axes. Specimens localised at the positive side of the axis are in black, the ones in the negative side are in grey.

affect the morphometric results, could be easily resolved with minor tuning of the photogrammetric protocol.

Photogrammetry offers a very low cost alternative to structured light surface scanning with a relatively short time needed for data acquisition, and using relatively basic equipment. Aside from the cost, accessibility and time efficiency, photogrammetry also captures the texture and colour of the objects in a more useful manner, allowing e.g. suture points to be more easily observed. Finally and perhaps most important in terms of the long-term curation and protection of important museum collections, photogrammetry will provide key accurate replica archives that can be shared and made more widely accessible for research.

Supplementary data to this article can be found online at http://dx.doi.org/10.1016/j.jasrep.2016.06.028.

Acknowledgements

We thank the Muséum National d'Histoire Naturelle, Paris, that provided access to the specimens, and access to the morphometric platform where the surface scans were performed. We also thank Raphael Cornette and Julien Claude for the fruitful discussions we had when writing the manuscript. This work was supported by NERC (grant number NE/K003259/1) and the European Research Council (ERC-2013-StG 337574-UNDEAD). This is publication **ISEM 2016-127**. We thank the two anonymous reviewers who greatly helped to improve the manuscript.

References

Adams, D.C., Otárola-Castillo, E., 2013. Geomorph: an <Scp > R</Scp > Package for the collection and analysis of geometric morphometric shape data. Methods Ecol. Evol. 4, 393–399. http://dx.doi.org/10.1111/2041-210X.12035.

Badawi-Fayad, J., Cabanis, E.A., 2007. Three-dimensional procrustes analysis of modern human craniofacial form. Anat. Rec. 290, 268–276.

Bates, K., Falkingham, P., Rarity, F., 2010. Application of high-resolution laser scanning and photogrammetric techniques to data acquisition, analysis and interpretation in palaeontology. Int. Arch. Photogramm. Remote Sens. Spat. Inf. Sci. XXXVIII 68–73.

Baylac, M., 2012. Rmorph: a R geometric and multivariate morphometrics library. (available on request at baylac@mnhn.fr).

Bookstein, F.L., 1997. Landmark methods for forms without landmarks: morphometrics of group differences in outline shape. Med. Image Anal. 1, 225–243.

Bouby, L., Figueiral, I., Bouchette, A., Rovira, N., Ivorra, S., Lacombe, T., Pastor, T., Picq, S., Marinval, P., Terral, J.-F., 2013. Bioarchaeological insights into the process of domestication of grapevine (*Vitis vinifera* L.) during Roman Times in Southern France. PLoS One 8, e63195. http://dx.doi.org/10.1371/journal.pone.0063195.

Boudadi-Maligne, M., Escarguel, G., 2014. A biometric re-evaluation of recent claims for Early Upper Palaeolithic wolf domestication in Eurasia. J. Archaeol. Sci. 45, 80–89. http://dx.doi.org/10.1016/j.jas.2014.02.006.

Cignoni, P., Corsini, M., Ranzuglia, G., 2008. MeshLab: an open-source 3D mesh processing system. ERCIM News 2008.

Counts, D.B., Walcek, Averett E., Garstki, K., 2016. A Fragmented Past: (Re) constructing Antiquity through 3D Artefact Modelling and Customised Structured Light Scanning at Athienou-Malloura, Cyprus. Antiquity 90, 206–218. http://dx.doi.org/10.15184/aqy.2015.181.

Cucchi, T., Hulme-Beaman, A., Yuan, J., Dobney, K., 2011. Early Neolithic pig domestication at Jiahu, Henan Province, China: clues from molar shape analyses using geometric morphometric approaches. J. Archaeol. Sci. 38, 11–22. http://dx.doi.org/10.1016/j.jas.2010.07.024.

Cucchi, T., Barnett, R., Martínková, N., Renaud, S., Renvoisé, E., Evin, A., Sheridan, A., Mainland, I., Wickham-Jones, C., Tougard, C., Quéré, J.P., Pascal, M., Pascal, M., Heckel, G., O'Higgins, P., Searle, J.B., Dobney, K.M., 2014. The changing pace of insular life: 5000 years of microevolution in the orkney vole (*Microtus arvalis orcadensis*). Evolution (N. Y) 68, 2804–2820. http://dx.doi.org/10.1111/evo.12476.

Cucchi, T., Kovács, Z.E., Berthon, R., Orth, A., Bonhomme, F., Evin, A., Siahsarvie, R., Darvish, J., Bakhshaliyev, V., Marro, C., 2013. On the trail of Neolithic mice and men towards Transcaucasia: zooarchaeological clues from Nakhchivan (Azerbaijan). Biol. J. Linn. Soc. 108, 917–928. http://dx.doi.org/10.1111/bij.12004.

Davis, S.J.M., 1981. The effects of temperature change and domestication on the body size of Late Pleistocene to Holocene mammals of Israel the effects of temperature change and domestication on the body size of Late Pleistocene to Holocene mammals of. Paleobiology 7, 101–114.

Drake, A.G., Coquerelle, M., Colombeau, G., 2015. 3D morphometric analysis of fossil canid skulls contradicts the suggested domestication of dogs during the late Paleolithic. Sci. Rep. 1–8. http://dx.doi.org/10.1038/srep08299.

Drake, A.G., Klingenberg, C.P., 2008. The pace of morphological change: historical transformation of skull shape in St Bernard dogs. Proc. Biol. Sci. 275, 71–76. http://dx.doi.org/10.1098/rspb.2007.1169.

Evin, A., Cucchi, T., Cardini, A., Strand Vidarsdottir, U., Larson, G., Dobney, K., 2013. The long and winding road: identifying pig domestication through molar size and shape. J. Archaeol. Sci. 40, 735–743. http://dx.doi.org/10.1016/j.jas.2012.08.005.

Evin, A., Flink, L.G., Blescu, A., Popovici, D., Andreescu, R., Bailey, D., Mirea, P., Lazr, C., Boronean, A., Bonsall, C., Vidarsdottir, U.S., Brehard, S., Tresset, A., Cucchi, T., Larson, G., Dobney, K., 2014. Unravelling the complexity of domestication: a case study using morphometrics and ancient DNA analyses of archaeological pigs from Romania. Philos. Trans. R. Soc. B Biol. Sci. 370, 20130616. http://dx.doi.org/10.1098/rstb.2013.0616.

Falkingham, P.L., 2012. Acquisition of high resolution three-dimensional models using free, open-source, photogrammetric software. Palaeontol. Electron. 15 (1T:15p).

Friess, M., 2012. Scratching the surface? The use of surface scanning in physical and paleoanthropology. J. Anthropol. Sci. 90, 7–31. http://dx.doi.org/10.4436/jass.90004.

Furukawa, Y., Ponce, J., 2010. Accurate, dense, and robust multiview stereopsis. IEEE Trans. Pattern Anal. Mach. Intell. 32, 1362–1376. http://dx.doi.org/10.1109/TPAMI.2009.161.

Goodall, C.R., 1995. Procrustes methods in the statistical analysis of shape revisited. In: Mardia, K.V., Gill, C.A. (Eds.), Current Issues in Statistical Shape Analysis. University of Leeds Press, Leeds, pp. 18–33.

Grosman, L., Smikt, O., Smilansky, U., 2008. On the application of 3-D scanning technology for the documentation and typology of lithic artifacts. J. Archaeol. Sci. 35, 3101–3110. http://dx.doi.org/10.1016/j.jas.2008.06.011.

Gunz, P., Mitteroecker, P., 2013. Semilandmarks: a method for quantifying curves and surfaces. Hystrix 24. http://dx.doi.org/10.4404/hystrix-24.1-6292.

Gunz, P., Mitteroecker, P., Bookstein, F.L., 2005. Semilandmarks in three dimensions. In: Academic, K. (Ed.), Modern Morphometrics in Physical Anthropology. Plenum, New York, New-York, pp. 73–98.

Hassett, B.R., Lewis-Bale, T., 2016. Comparison of 3D landmark and 3D dense cloud approaches to Hominin mandible morphometrics using Structure-From-Motion. Archaeometry http://dx.doi.org/10.1111/arcm.12229.

Haukaas, C., Hodgetts, L.M., 2016. The untapped potential of low-cost photogrammetry in community-based archaeology: a case study from Banks Island. Arctic Canada. J. Community Archaeol. Herit. 3, 40–56.

Katz, D., Friess, M., 2014. Technical note: 3D from standard digital photography of human crania-a preliminary assessment. Am. J. Phys. Anthropol. 154, 152–158. http://dx.doi.org/10.1002/ajpa.22468.

Kolamunnage, R., Kent, J.T., 2003. Principal component analysis for shape variation about an underlying symmetric shape. In: Aykroyd, R.G., Mardia, K.V., Langdon, M.J. (Eds.), Stochastic Geometry, Biological Structure and Images. Leeds University Press, Leeds, pp. 137–139.

Lowe, D.G., 1999. Object recognition from local scale-invariant features. Proc. Seventh IEEE Int. Conf. Comput. Vis. 2, 1150–1157. http://dx.doi.org/10.1109/ICCV.1999.790410.

Mcpherron, S.P., Gernat, T., Hublin, J., 2009. Structured light scanning for high-resolution documentation of in situ archaeological finds. J. Archaeol. Sci. 36, 19–24. http://dx.doi.org/10.1016/j.jas.2008.06.028.

Monteiro, L.R., 1999. Multivariate regression models and geo-metric morphometrics: the search for causal factors in the analysis of shape. Syst. Biol. 48, 192–199.

Morey, D.F., 1992. Size, shape and development in the evolution of the domestic dog. J. Archaeol. Sci. 19, 181–204. http://dx.doi.org/10.1016/0305-4403(92)90049-9.

Newton, C., Lorre, C., Sauvage, C., Ivorra, S., Terral, J.F., 2014. On the origins and spread of *Olea europaea* L. (olive) domestication: evidence for shape variation of olive stones at Ugarit, Late Bronze Age, Syria-a window on the Mediterranean Basin and on the westward diffusion of olive varieties. Veg. Hist. Archaeobot. 23, 567–575. http://dx.doi.org/10.1007/s00334-013-0412-4.

Núñez, M.A., Buill, F., Edo, M., 2013. 3D model of the Can Sadurní cave. J. Archaeol. Sci. 40, 4420–4428. http://dx.doi.org/10.1016/j.jas.2013.07.006.

Pagnoux, C., Bouby, L., Ivorra, S., Petit, C., Valamoti, S.M., Pastor, T., Picq, S., Terral, J.F., 2014. Inferring the agrobiodiversity of *Vitis vinifera* L. (grapevine) in ancient Greece by comparative shape analysis of archaeological and modern seeds. Veg. Hist. Archaeobot. 24, 75–84. http://dx.doi.org/10.1007/s00334-014-0482-y.

Pavlidis, G., Koutsoudis, A., Arnaoutoglou, F., Tsioukas, V., Chamzas, C., 2007. Methods for 3D digitization of Cultural Heritage. J. Cult. Herit. 8, 93–98. http://dx.doi.org/10.1016/j.culher.2006.10.007.

Porter, S.T., Roussel, M., Soressi, M., 2016. A simple photogrammetry rig for the reliable creation of 3D artifact models in the field lithic examples from the early upper Paleolithic sequence of Les Cottés (France). Adv. Archaeol. Pract. 4, 71–86.

R Core Team, R.C.T., 2014. R: A Language and Environment for Statistical Computing.

Rohlf, F.J., Slice, D., 1990. Extensions of the procrustes method for the optimal superimposition of landmarks. Syst. Biol. 39, 40–59.

Ros, J., Evin, A., Bouby, L., Ruas, M.-P., 2014. Geometric morphometric analysis of grain shape and the identification of two-rowed barley (*Hordeum vulgare* subsp. *distichum* L.) in southern France. J. Archaeol. Sci. 41, 568–575. http://dx.doi.org/10.1016/j.jas.2013.09.015.

Sapirstein, P., 2016. Accurate measurement with photogrammetry at large sites. J. Archaeol. Sci. 66, 137–145.

Seetah, T.K., Cardini, A., Miracle, P.T., 2012. Can morphospace shed light on cave bear spatial-temporal variation ? Population dynamics of Ursus spelaeus from Romualdova pe cina and Vindija, (Croatia). J. Archaeol. Sci. 39, 500–510. http://dx.doi.org/10.1016/j.jas.2011.10.005.

Sholts, S.B., Flores, L., Walker, P.L., Wärmländer, S.K.T.S., 2011. Comparison of coordinate measurement precision of different landmark types on human crania using a 3D laser scanner and a 3D digitiser: implications for applications of digital morphometrics. Int. J. Osteoarchaeol. 21, 535–543.

Souter, T., Cornette, R., Pedraza, J., Hutchinson, J., Baylac, M., 2010. Two applications of 3D semi-landmark morphometrics implying different template designs: the theropod pelvis and the shrew skull. Comptes Rendus Palevol 9, 411–422. http://dx.doi.org/10.1016/j.crpv.2010.09.002.

Tchernov, E., Kolska Horwitz, L., 1991. Body size diminution under domestication: unconscious selection in primeval domesticates. J. Anthropol. Archaeol. 10, 54–75. http://dx.doi.org/10.1016/0278-4165(91)90021-O.

Terral, J.-F., Tabard, E., Bouby, L., Ivorra, S., Pastor, T., Figueiral, I., Picq, S., Chevance, J.-B., Jung, C., Fabre, L., Tardy, C., Compan, M., Bacilieri, R., Lacombe, T., This, P., 2010. Evolution and history of grapevine (*Vitis vinifera*) under domestication: new morphometric perspectives to understand seed domestication syndrome and reveal origins of ancient European cultivars. Ann. Bot. 105, 443–455. http://dx.doi.org/10.1093/aob/mcp298.

Verhoeven, G., Doneus, M., Briese, C., Vermeulen, F., 2012. Mapping by matching: a computer vision-based approach to fast and accurate georeferencing of archaeological aerial photographs. J. Archaeol. Sci. 39, 2060–2070. http://dx.doi.org/10.1016/j.jas.2012.02.022.

Wayne, R.K., 1986. Cranial morphology of domestic and wild canids : the influence of development on morphological change. Evolution (N. Y) 40, 243–261.

Weinberg, S.M., Naidoo, S.D., Bardi, K.M., Brandon, C.A., Neiswanger, K., Resick, J.M., 2009. Face shape of unaffected parents with cleft affected offspring: combining three-dimensional surface imaging and geometric morphometrics. Orthod Carniofac Res. 12, 271–281. http://dx.doi.org/10.1111/j.1601-6343.2009.01462.x.Face.

Wu, C., 2013. Towards Linear-Time Incremental Structure from Motion. 2013 International Conference on 3D Vision, pp. 127–134 http://dx.doi.org/10.1109/3DV.2013.25 IEEE.

Wu, C., 2011. VisualSFM: A visual structure from motion system [WWW document]http://ccwu.me/vsfm/.

Wu, C., 2007. SiftGPU : A GPU Implemention of Scale Invariant Feature Transform (SIFT) [WWW Document].

Wu, C., Agarwal, S., Curless, B., Seitz, S.M., 2011. Multicore bundle adjustment. Comput. Vis. Pattern Recognit. (CVPR), 2011 IEEE Conf. 3057–3064 http://dx.doi.org/10.1109/CVPR.2011.5995552.

Yamafune, K., Torres, R., Castro, F., 2016. Multi-image photogrammetry to record and reconstruct underwater shipwreck sites. J. Archaeol. Method Theory 1–23 http://dx.doi.org/10.1007/s10816-016-9283-1.